THE JOURNAL OF PHYSICAL CHEMISTRY B
A JOURNAL OF THE AMERICAN CHEMICAL SOCIETY

pubs.acs.org/JPCB Article

Quantifying Long-Time Hydrogen−Deuterium Exchange of Bovine Serum Albumin with Hydrogen−Deuterium Exchange Small-Angle Neutron Scattering

Róisín B. Donnelly, Norman J. Wagner,* and Yun Liu*

Cite This: https://doi.org/10.1021/acs.jpcb.4c03967 Read Online

ACCESS | Metrics & More | Article Recommendations | Supporting Information

ABSTRACT: Hydrogen−deuterium exchange (HDX) measured by small-angle neutron scattering (HDX-SANS) is used to measure HDX in bovine serum albumin (BSA) under different temperatures and formulation conditions. HDX-SANS measurements are performed at 40, 50, and 60 °C in D_2O after storing proteins at 4 °C for 1 week to pre-exchange the readily accessible hydrogens. This enables us to probe the long-time HDX of protons at the core of the BSA proteins, which is more challenging for solvent molecules to access. The HDX kinetics are observed to follow an Arrhenius behavior with an apparent activation energy of 81.4 ± 1 kJ/mol, which is composed of the energy for protein conformational fluctuations and that for exchanging an amide hydrogen. Adding a tonicity agent of 150 mM NaCl has only a very slight effect on the HDX kinetics. Interestingly, we also observed that the formulation with faster HDX kinetics has a lower onset temperature of denaturation. This observation is qualitatively consistent with a previous study of HDX-SANS on a monoclonal antibody (mAb), despite the large difference of the secondary structure between BSA, dominated by alpha helices, and mAb, which is predominantly composed of β-sheets.

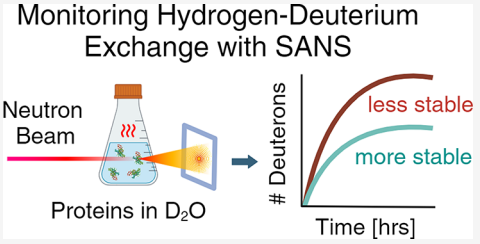

INTRODUCTION

The biopharmaceutical industry has experienced unprecedented success with protein-based drugs, particularly monoclonal antibodies (mAbs), resulting in multibillion-dollar sales.[1] Although mAb-based drugs hold promise for therapeutic applications, their advancement and widespread adoption still have many challenges, such as the limited understanding of their long-term stability and shelf life.[2−4]

Hydrogen−deuterium exchange (HDX) has been identified as a potential method for predicting the long-term stability of mAbs.[5,6] By measuring the exchange kinetics of labile hydrogens in the protein's amide groups with deuterium from the deuterium oxide-based buffer, HDX provides insights into conformational fluctuations present in proteins. Labile protons on the protein surface can undergo HDX in as little as a few milliseconds. However, a much slower exchange of hydrogen occurs over many hours to days. This long-time HDX, which is potentially related to protein instability, is possible only when the more deeply buried labile hydrogens of the protein become solvent-accessible due to conformational fluctuations.[7,8] These naturally occurring conformational fluctuations have been correlated with long-term physical and chemical instability, and therefore, quantifying the rate of such conformational fluctuations could be useful in predicting shelf life.[6] Thus, HDX is a promising approach for enhancing our understanding of protein stability in formulations, which can help accelerate the production of therapeutic proteins.

Mass spectrometry (MS) is commonly used for measuring HDX, and this method offers insights into the conformational fluctuations of proteins through identification of the HDX position within the peptide sequence.[9−14] In this method, samples are removed from the solution and processed for measurement at specific time points. Nuclear magnetic resonance (NMR) tracks HDX by leveraging the difference of chemical shifts between hydrogen and deuterium, offering amino acid-level resolution.[15−17] IR and Raman spectroscopy are alternative approaches that monitor HDX by detecting vibrational changes associated with HDX.[18,19] Recently, hydrogen−deuterium exchange small-angle neutron scattering (HDX-SANS) has been proposed as a sensitive, non-destructive, and complementary approach for assessing HDX directly in protein formulations.[2] With a simple experimental setup, HDX-SANS allows for real-time, noninvasive measurement of protein HDX in liquid formulations and offers insights into the spatial distribution of exchanged hydrogens from a higher-order structural perspective.[2] Furthermore, HDX-SANS can explore in situ HDX under various conditions such as pressure, shear, or chemical stimuli, taking advantage of

Received: June 17, 2024
Revised: November 10, 2024
Accepted: November 12, 2024

advanced SANS sample environments.[20] Despite its many advantages, HDX-SANS faces limitations, particularly the restricted access to suitable neutron sources, which makes it difficult to use as a routine analysis method. Additionally, the required counting time, such as 15 min for a single SANS pattern used in this study, limits the time resolution for HDX-SANS measurements. Nonetheless, HDX-SANS provides valuable quantitative information that enhances the validation and deepens the understanding of complementary techniques, such as HDX-NMR and HDX-MS.

Prior HDX-SANS work on mAbs has provided valuable insights into the influence of formulation conditions, particularly in the presence of sodium salts of varying degrees of interaction with the mAb, on the HDX kinetics of NISTmAb.[2] These investigations highlighted the strong correlation between the effect of strongly kosmotropic or strongly chaotropic salts on the HDX and the thermal stability of mAb formulations, thereby proving that the long-time HDX accessible by SANS is a measure of protein thermal stability in formulation.[2] However, because HDX is influenced by the secondary structure of proteins,[21,22] it is relevant to expand the exploration of HDX-SANS to proteins with different secondary structures.

In this work, we build upon the previous HDX-SANS study of NIST monoclonal antibody,[2] to investigate the impact of multiple temperatures, in addition to buffer conditions, on the long-time HDX kinetics of bovine serum albumin (BSA). BSA has a secondary structure significantly different from mAbs. While mAbs are dominated by β-sheets, the secondary structure of BSA has no β-sheets and is dominated by α-helices, with about 67% α-helix, 10% turn, and 23% extended chain configurations.[23] Additionally, BSA, which is a globular protein, holds significant importance both physiologically and as a model system in the field of biophysical chemistry.[24−29]

In this study, we focus on examining the long-time HDX kinetics of bovine serum albumin (BSA) at temperatures of 40, 50, and 60 °C, enabling the determination of an activation energy for HDX in BSA in D_2O. We anticipate that elevated temperatures will yield enhanced HDX.[30] By measuring the temperature-dependent HDX, we demonstrate here that HDX-SANS can be used to extract the activation energy. Furthermore, the present work explores the impact of sodium chloride on the HDX of BSA measured at 60 °C. Sodium chloride is composed of both weakly kosmotropic (Na+) and weakly chaotropic (Cl−) ions[31] and is commonly used in protein drug formulation as a tonicity or viscosity modifier.[32−34] Even though the addition of 150 mM sodium chloride is not expected to have a large impact on HDX, the HDX-SANS is sensitive to observing the difference of the HDX kinetics. This underscores the utility of HDX-SANS as a robust screening tool capable of detecting subtle differences in the HDX kinetics among protein formulation options. By performing HDX-SANS on BSA, we verified the technique as a sensitive, noninvasive method.

MATERIALS AND METHODS

Sample Preparation. Lyophilized bovine serum albumin was obtained from Sigma-Aldrich (product number A7638) and dissolved in buffer composed of either deuterium oxide (D_2O) or D_2O with 150 mM sodium chloride, aided by 10 s of gentle vortex mixing and 30 min of mixing on a horizontal rolling mixer at a low speed. Samples were stored at 4 °C for 5−7 days prior to SANS measurements. By allowing the hydrogenated protein samples to sit in the D_2O-based buffer for 5−7 days prior to the experiment, all the readily exposed labile hydrogens are assumed to have undergone HDX. Aliquots of both samples, with and without sodium chloride, were diluted and set aside and stored at 4 °C for differential scanning calorimetry experiments. The pH of the samples is neutral and not greatly impacted by the protein concentration or the presence of sodium chloride. The pH range of all samples was 6.6 ± 0.5, which agrees with the pH measurements of Zhang et al. (2012).[35]

Differential Scanning Calorimetry. Differential scanning calorimetry was performed with a NanoDSC instrument (TA Instruments, Newcastle, DE). Prior to the experiment, this instrument was cleaned by first soaking the capillary with 5% Contrad for 1 h and then flushing with 2 L of Milli-Q water. Three buffer scans were performed, each of which consisted of both heating and cooling steps from 25 to 110 °C at a rate of 1 °C/min. Following buffer measurements, BSA protein samples (1 or 2 mg/mL) were loaded, and the heat capacity was measured over the same temperature range and rate. All measurements were performed at a constant pressure of 3 atm. The resultant thermograms were corrected with the buffer scan and fit to a single Gaussian model in Nano Analyze software (TA Instruments). From the fit thermogram, the onset temperature of denaturation, melting temperature, and change in enthalpy (ΔH) were determined.

Hydrogen−Deuterium Exchange SANS (HDX-SANS). Hydrogen−deuterium exchange small-angle neutron scattering measurements were performed at the NGB 30m SANS beamline at the Center for Neutron Research of the National Institute of Standards and Technology beamline. After filtering with a 0.1 μm pore size polyvinylidene difluoride membrane syringe filter, approximately 1 mL of sample was loaded into 2 mm-thick quartz banjo cells. Each sample at 100 mg/mL BSA concentration was measured first at 10 °C and then elevated to its target temperature of either 40, 50, or 60 °C. Once the sample reached its target elevated temperature, it was measured by SANS continually for the duration of the kinetics experiment. Upon the completion of the kinetics experiment, the sample temperature was reduced again to 10 °C and a SANS pattern was measured again. The final 10 °C measurement can be utilized to estimate the amount of exchange that occurred during heating to the target elevated temperature, as described by Donnelly et al. (2023).[2] Each SANS pattern measurement took 15 min. For all samples, the detector was placed at 4 m to obtain a Q-range from 0.01 to 0.045 Å^{-1}. Additionally, at least one measurement was also used at the detector distance of 1 m to measure high Q values, which allow us to extract the incoherent background. A low concentration sample (10 mg/mL) was also measured at 10 °C to extract the initial scattering length density of BSA in D_2O.

HDX-SANS Analysis. SANS measures the scattering intensity as a function of the scattering vector, $\vec{Q}$. For solution samples, the scattering intensity is usually isotropic and is a function of the magnitude of $\vec{Q}$, which is defined as

$$Q = \frac{4\pi}{\lambda}\sin\left(\frac{\theta}{2}\right) \quad (1)$$

where λ is the wavelength and θ is the scattering angle. Once corrected for the incoherent and Q-independent background (B), the coherent scattering intensity, $I(Q)$, for monodisperse particles can be expressed as

https://doi.org/10.1021/acs.jpcb.4c03967
J. Phys. Chem. B XXXX, XXX, XXX−XXX

$$I(Q) = I_m(Q) - B = nV_p^2(\Delta\rho)^2\tilde{P}(Q)S(Q) \quad (2)$$

where $I_m(Q)$ is the scattering intensity from a sample and B represents the background that is mostly dominated by the incoherent scattering. The contrast term $\Delta\rho$ is the difference of the scattering length density (SLD) between the particle and solvent, n is the particle number density, and V_p is the volume of an individual particle. $\tilde{p}(Q)$ is the normalized form factor, which is solely determined by the particle structure, and $S(Q)$ is the interparticle structure factor. This expression assumes a monodisperse suspension of spherical particles in solution. If the scattering length density distribution of particles are not isotropic, $S(Q)$ should be considered as an effective structure factor.[36,37]

HDX-SANS analysis was performed following the procedure outlined in Donnelly et al. (2023) to produce the SANS pattern ratios, $R(Q)$.[2] In this method, a ratio of temporal SANS patterns is used as the primary result for analysis, as

$$R(Q) = \frac{I(Q)_t}{I(Q)_{t=0}} = \frac{nV_p^2(\Delta\rho_t)^2\tilde{P}(Q)_t S(Q)}{nV_p^2(\Delta\rho_{t=0})^2\tilde{P}(Q)_{t=0}S(Q)} = \frac{(\Delta\rho_t)^2\tilde{P}(Q)_t}{(\Delta\rho_{t=0})^2\tilde{P}(Q)_{t=0}} \quad (3)$$

In the above eq 3, the subscript $t = 0$ refers to the first SANS measurement and t indicates the starting time of acquisition of the SANS pattern of interest at all later times. Here, we assume that structure factor $S(Q)$ is independent of HDX for the 100 mg/mL BSA samples.

Further analysis was performed on $R(Q)$ within the intermediate Q-range (0.03 to 0.08 Å^{-1}), which was optimized to prevent the influence of noise, background subtraction, and any potential aggregate formation on the analysis. More details regarding the rationale for this Q-range selection are provided in the Supporting Information.

If the change in scattering length density is not uniform throughout the protein, i.e., the HDX does not occur uniformly across a protein, it could lead to the change of the normalized form factor $\tilde{p}(Q)$ at different times. Thus, in principle, from the Q-dependent trend of $R(Q)$, the location of HDX could be inferred. However, given the relative percentage of exchangeable hydrogens in the fluctuating protein and the angular averaged nature of the SANS measurement, the form factor changes are anticipated to be small.

If Q is within the Guinier region, $R(Q)$ can be further simplified as

$$R(Q) \approx \left(\frac{(\Delta\rho_t)^2 e^{-1/3Q^2r_t^2}}{(\Delta\rho_{t=0})^2 e^{-1/3Q^2r_{t=0}^2}}\right) \quad (4)$$

which leads to

$$\ln R(Q) \approx 2\ln y - \frac{1}{3}(\Delta(r^2))Q^2 \quad (5)$$

where y represents the contrast term, $\left|\frac{\Delta\rho_t}{\Delta\rho_{t=0}}\right|$ and

$$\Delta(r^2) = r_t^2 - r_{t=0}^2 \quad (6)$$

where $r_{t=0}$ is the radius of gyration of BSA at the beginning of the HDX kinetics measurement while r_t is the radius of gyration at the later time point in measurement, which may change slightly as HDX occurs. Note that HDX is not expected to change the physical radius of the protein, but a change in the radius detected by SANS can occur if HDX is not uniformly distributed throughout the protein. This enables a qualitative discussion of the relative location of HDX provided that a positive trend in $\Delta(r^2)$ values indicates that more exchanges occur in the core of the protein, while a negative trend of $\Delta(r^2)$, would indicate more HDX is occurring on the shell of the protein. If $\Delta(r^2)$ is neither positive nor negative, but hovering around 0, this indicates that HDX is likely uniform throughout the protein, which is the case for BSA in D_2O. Though HDX was mostly uniform throughout BSA, this analysis could be beneficial for the study of the relative distribution of HDX in other proteins in future works. Additionally, this linear fitting (eq 5) also enables determination of y, related to HDX kinetics. The values of y from $R(Q)$ were plotted as a function of time to yield the HDX kinetics, similar to our prior HDX-SANS work.[2] As in the previous study, the change in contrast can be modeled using the following result assuming a pseudo-first-order exchange kinetics relationship with a background related to unexchangeable hydrogens in a protein:

$$y = \bar{y}_\infty + (1 - \bar{y}_\infty)e^{-t/\tau} \quad (7)$$

The parameter τ is the characteristic exchange time of HDX, and $\bar{y}_\infty$ is the asymptotic value of y at an infinite waiting time. From the exchange time parameter, τ, an overall activation energy for the HDX process can be calculated from the Arrhenius equation as follows:

$$\tau = Ae^{E_a/RT} \quad (8)$$

where E_a is the activation energy, R is the gas constant, A is the prefactor, and T is the absolute temperature in Kelvin.

As SANS is a quantitative measure of the total scattering, the number of deuterons incorporated into the BSA samples during the SANS measurement can be calculated following the procedure of Donnelly et al. (2023)[2] using the relationship

$$n_{HDX} = \frac{V_p(y-1)(\rho_{protein_{t=0}} - \rho_{solvent})}{b_D - b_H} \quad (9)$$

where V_p represents the volume of one BSA protein, which has been reported as 81,200 Å^3.[35] The value of $\rho_{protein_{t=0}}$ was determined to be $(3.3 \pm 0.5) \times 10^{-6}$ Å^{-2} from an ellipsoid form factor fitting, and this represents SLD at the beginning of the HDX-SANS experiment. This value is similar to what has been reported in the literature.[35,38] $\rho_{solvent}$ is the scattering length densities for the solvent (i.e., D_2O or D_2O with 150 mM sodium chloride), and b_D and b_H are the bound coherent scattering lengths of deuterium (6.671 fm) and hydrogen (−3.7390 fm), respectively.

RESULTS AND DISCUSSION

DSC measurements of BSA with and without sodium chloride resulted in single-peak thermograms (Figure 1) consistent with similar studies of BSA at comparable pH levels.[39] The melting temperature for BSA in D_2O was approximately 71 °C and the onset temperature, marked by a noticeable uptick in the DSC signal, occurred at ≈56 °C (Table 1). Adding 150 mM sodium

https://doi.org/10.1021/acs.jpcb.4c03967
J. Phys. Chem. B XXXX, XXX, XXX−XXX

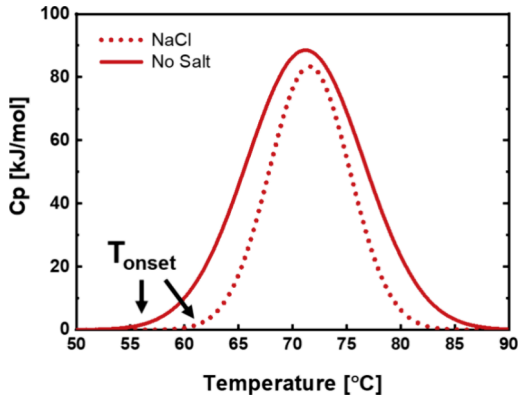

Figure 1. DSC thermograms for BSA protein in D_2O (No Salt, solid line) and D_2O with 150 mM NaCl (NaCl, dotted line). Each DSC profile is measured in triplicate, and one representative thermogram is depicted herein.

Table 1. Onset Temperature of Denaturation, Melting Temperature, and Enthalpy of Denaturation for BSA Samples Obtained from the DSC Thermograms

formulation conditions (1 mg/mL BSA)	onset temperature [°C]	melting temperature [°C]	enthalpy ΔH [kJ/mol]
D_2O	56 ± 1	71 ± 1	1195 ± 12
D_2O + 150 mM NaCl	62 ± 1	72 ± 1	1080 ± 7

chloride slightly increases the onset temperature to 62 °C. The overall melting temperature seems to be also shifted slightly to 72 °C, but the difference is within measurement uncertainty (Table 1). This result agrees with a previous study on the thermal stability of BSA assessed by DSC.[40] This suggests that sodium chloride slightly enhances the thermal stability by slightly shifting the onset temperature. The melting enthalpy values for the BSA samples are around 1100 kJ/mol based on the Gaussian model fit of the thermograms (Table 1).

A low concentration sample (10 mg/mL BSA) without the addition of salt (Figure 2 A) was measured at a low temperature (10 °C) to estimate the SLD of BSA in D_2O. This value of SLD is needed to extract the number of exchanged hydrogens of BSA proteins during the HDX-SANS experiments. At the dilute condition, the scattering pattern is dominated by the form factor. The solid line in Figure 2A is the resultant form factor fitting curve using an ellipsoid model provided in the software, SasView. The size of the BSA protein, determined from the fitting, is consistent with a previous work by Zhang et al. (2012) and reported in Table 2.[35] The extracted SLD of BSA is $(3.3 \pm 0.5) \times 10^{-6}$ Å^{-2} (Figure 2A), which is also consistent with a literature result.[35]

Concentrated samples (100 mg/mL) of BSA are used here for the HDX-SANS experiments, as the stronger signals from concentrated proteins can help improve the time resolution of the HDX-SANS experimental measurements. All samples were measured at 10 °C prior to the thermal kinetics HDX-SANS measurements (Figure 2B,C). For the sample without salt, there is a prominent structure factor peak at around $Q \sim 0.05$ Å^{-1} due to the strong repulsion between proteins (Figure 2B). The addition of salt increases the ionic strength and screens the electrostatic repulsions between the proteins, leading to less repulsive interactions and a less prominent structure factor peak (Figure 2C).

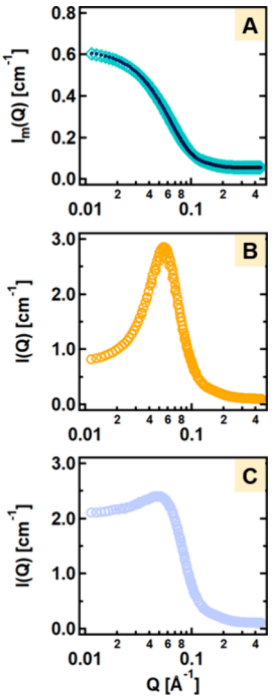

Figure 2. SANS patterns acquired at 10 °C, prior to high temperature exposure, of (A) a low concentration sample (10m g/mL) of BSA protein in D_2O (teal), with the form factor fitting line eq 2 overlaid (black line), (B) 100 mg/mL BSA in D_2O, and (C) 100 mg/mL BSA in D_2O with 150 mM sodium chloride.

Table 2. Fitting Parameters of the Form Factor for BSA in D_2O

SLD of solvent (Å^{-2})	6.335×10^{-6}
SLD of protein (Å^{-2})	$(3.3 \pm 0.5) \times 10^{-6}$
polar radius (Å)	12.5 ± 0.2
equatorial radius (Å)	41 ± 1.1

Kinetics HDX-SANS measurements were collected on three identical BSA samples (100 mg/mL) at three different temperatures, 40, 50, or 60 °C, without any added salts. The SANS patterns obtained at each of these elevated temperatures display a similar trend with a consistent downward shift in the SANS intensity with time without any significant change in the pattern shape. This trend is more evident in the inset of each panel in Figure 3. A small change in the scattering length density of the protein toward that of the solution (D_2O), induced by HDX, should not have a significant effect on the pattern itself. Instead, it should gradually reduce the contrast over time, resulting in a uniformly decreasing scattering intensity.

$R(Q)$ was calculated from the measurements in Figure 3 using eq 4 and is plotted in Figure 4. The selected Q-range for ratio analysis (0.03 to 0.08 Å^{-1}) is delineated by dotted lines in Figure 3 and was optimized based on the relative intensity of SANS and any potential influence of aggregate formation on the results. (See the SI for the detailed discussion.)

Over the observation time, the values of $R(Q)$ for all three samples decrease, consistent with anticipated trends observed in Figure 4. The time resolution is limited by the time needed to collect one SANS pattern with sufficient statistics, which is 15 min. Only a few selected data are shown in Figure 4 for clarity. As HDX proceeds, the average SLD of the protein

https://doi.org/10.1021/acs.jpcb.4c03967
J. Phys. Chem. B XXXX, XXX, XXX−XXX

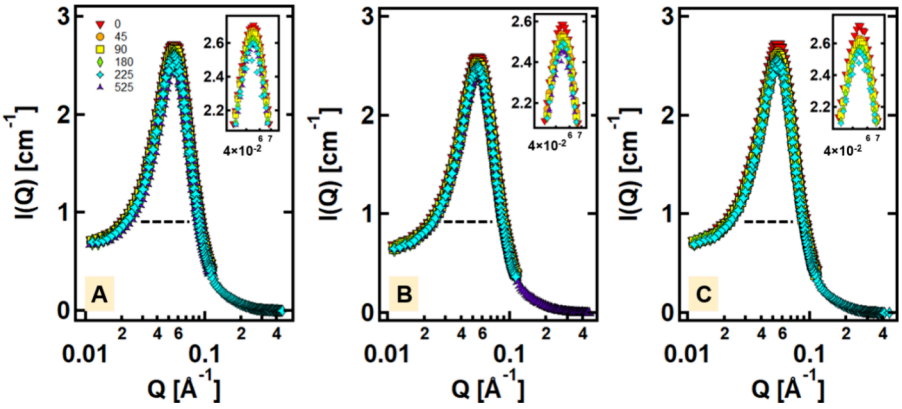

Figure 3. SANS patterns acquired over time elapsed from 0 to 225 min of 100 mg/mL BSA exposed to (A) 40 °C, (B) 50 °C, and (C) 60 °C. Measurement time for each SANS pattern is 15 minutes. Inset plots highlight the uniform drop of SANS pattern intensity across all samples. There is a drop in the SANS pattern with time as denoted by the color scheme from 0 to 45 min, ···, to 225 min (red, orange, ···, teal). The time legend is consistent across different sample types. The black dashed horizontal lines delineate the Q range selected for the ratio analysis (0.03 to 0.08 Å^{-1}).

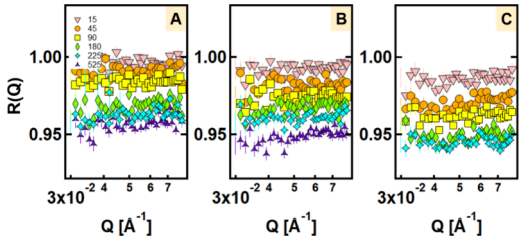

Figure 4. Plots of $R(Q)$, the SANS pattern ratios produced by dividing SANS patterns at later times with $I(Q)_{t=0}$, which is the first SANS pattern acquired. This was performed for each 100 mg/mL BSA sample exposed to (A) 40 °C, (B) 50 °C, and (C) 60 °C. The color-coded legend represents the time elapsed for each sample from 15 min (peach downward triangle), 45 min (orange circle), 90 min (yellow square), etc. The legend is consistent across the three temperature plots. There is a drop in the value of $R(Q)$ with increased time in each sample condition from 15 min (peach downward triangle) to 225 min (teal diamond).

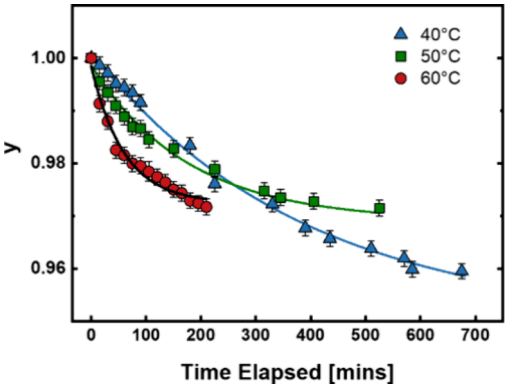

Figure 5. y, extracted by fitting of $R(Q)$, for BSA samples exposed to 40 °C (blue triangle), 50 °C (green square), and 60 °C (red circle), is plotted as a function of the time elapsed. Over time, the values of y decrease, indicating the loss of scattering contrast, which is caused by the HDX. The lines running through the data points represent model fitting with eq 7. The values of the data points plotted herein can be found in Table S1 in the Supporting Information.

increases. As a result, the contrast difference between the proteins and D_2O, $(\Delta\rho)^2$, in eq 2 becomes smaller. Thus, the SANS intensity decreases over time, resulting in $R(Q)$ decreasing. At 225 min, the $R(Q)$ for the sample at 60 °C is the smallest among all three temperatures. Thus, a higher temperature accelerates the HDX, as expected. Although this qualitative analysis of the $R(Q)$ results supports our hypothesis, a more quantitative analysis, (discussed below), is necessary to fully understand differences in the HDX dynamics with temperature.

By taking a ratio of SANS measurements, the effect of the interparticle structure factor, $S(Q)$, is removed by assuming that the HDX does not influence $S(Q)$. Any change in $R(Q)$ is due to the contrast and the change in the hydrogen distribution due to the HDX. Equation 5 is used to extract the relative contrast change, $y = \left|\frac{\Delta\rho_t}{\Delta\rho_{t=0}}\right|$. The parameter y was determined from fitting the data collected in the indicated time interval, with an example of the fit provided for the ratios corresponding to 15 min elapsed, shown in Figure S2 in the Supporting Information. The ratios are quite flat in the studied Q-range, indicating that the overall hydrogen distribution of the proteins is still relatively uniform.

The values of y were calculated and plotted as a function of elapsed time, as depicted in Figure 5, while the corresponding fit parameters are presented in Figure 6 and in Table S1 in the Supporting Information. The temperature has a measurable impact on HDX with higher temperatures resulting in faster HDX. The initial decay rate, reflecting the exchange rate, is

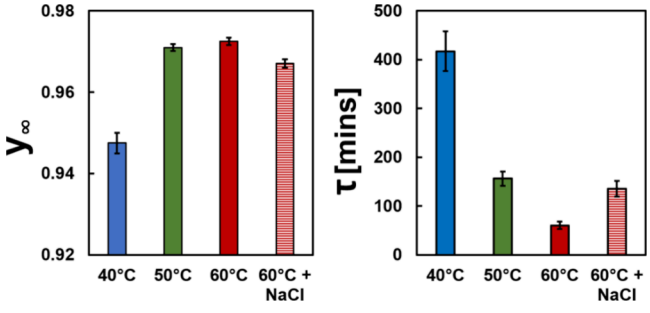

Figure 6. Summary of the fitting parameters obtained for the model fit of y. The values of y_∞ shown in the left are related to the percent of hydrogens present in each sample, if they were allowed infinite HDX time at their respective elevated temperatures, while τ, in the right, corresponds to the characteristic exchange time of HDX for each sample.

https://doi.org/10.1021/acs.jpcb.4c03967
J. Phys. Chem. B XXXX, XXX, XXX−XXX

greatest in the sample exposed to 60 °C, followed by that at 50 °C, and slowest at 40 °C. This result supports the hypothesis that faster exchange would occur at higher temperatures. The empirical fit of data presented in Figure 5 also enables the extraction of the characteristic time of exchange, τ, which is inversely proportional to the rate of HDX taking place in a sample. This characteristic time changes from about 400 min at 40 °C to about 60 min at 60 °C. Thus, the rate of HDX is nearly seven times slower at 40 °C than that at 60 °C. Overall, τ indicates that the rate of exchange increases with increasing temperature, as was anticipated. Each fitting line (Figure 5), which produced the values of τ and y_∞, had an R^2 value between 0.97 to 0.99, and the residuals of these fits can be found in the Figure S3 in the Supporting Information.

The empirical fit of the kinetics includes an asymptotic value y_∞, related to the plateau in exchange at a long time. In this analysis, $1 - y_\infty$ is related to the fraction of exchange relative to the number of hydrogens at the start of the SANS measurement, and this is detailed in the Table S2 in the Supporting Information. The y_∞ parameter is related to be the fraction of hydrogens that are unexchanged in a protein compared with the total number of exchangeable hydrogen at t = 0 min, where t = 0 refers to the first SANS measurement at temperature.[2] Note that y_∞ is almost the same for samples at both 50 and 60 °C, while it is smaller for the sample at 40 °C. This is due to the normalization based on initial measurements at high temperatures. Some HDX already takes place as the samples are heated to the target temperatures (40, 50, or 60 °C). It is estimated at the later part of the paper that there is less hydrogen exchange during the heating at 40 °C than at 50 and 60 °C, resulting in fewer hydrogens available for exchange at 50 and 60 °C of the subsequent kinetics measurements. In other words, each BSA sample starts the high-temperature kinetics measurements with a different number of hydrogens remaining for exchange, depending on the heating temperature. Note that the hydrogen exchange during the heating does not affect the result of τ obtained at 40, 50, or 60 °C.

The value of the apparent activation energy for HDX of 84.1 ± 1 kJ/mol is determined from an Arrhenius plot of the time constants, τ, (Figure 7). The data follow the expected Arrhenius behavior. The interpretation of this activation energy value can be guided by the HDX model, which was originally proposed by Linderstrom−Lang and has since been discussed extensively.[30,41,42] Three exchange rate parameters determine the observed kinetics of the HDX: the rate of a protein opening its closed structure, k_{op}; the rate of a protein closing its opened structure, k_{cl}; and the chemical exchange rate of the accessible amide, k_{ch}.[30] If $k_{ch} \gg k_{cl}$, the HDX is considered the EX_1 kinetics. If $k_{ch} \ll k_{cl}$, it is considered as the EX_2 kinetics. For most protein systems, it is rare to have EX_1 kinetics and more common to observe EX_2 kinetics,[30] and in some cases, a combination of the two kinetics regimes is possible.[43,44] For EX_1 kinetics, the apparent energy extracted from the temperature-dependent data is the activation energy needed to open the protein secondary structure to expose its internal hydrogen. Although the kinetics regimes of the BSA samples in this experiment are unknown and further research is needed to understand the relationship between temperature and these kinetics regimes,[45] if all BSA samples were to follow purely EX_1 kinetics, the extracted activation energy of 84.1 ± 1 kJ/mol would correspond to the energy needed to unfold its secondary structure. For an EX_2 process, the apparent activation energy is influenced by two terms: one is the free energy of the local stability, and the additional contribution is the energy needed to exchange hydrogen and deuterium at an open amide site. The latter is reported to be around 14 kcal/mol (58.6 kJ/mol), 17 kcal/mol (71.1 kJ/mol), and 19 kcal/mol (79.5 kJ/mol) in acid, base, and neutral water, respectively.[30] For EX_2 kinetics, our experimental activation energy (84.1 ± 1 kJ/mol) minus the energy needed to exchange hydrogen and deuterium at an open amide site in neutral water (79.5 kJ/mol) is around 5 kJ/mol. This is consistent with the hydrogen bonding energy between amide− amide in a protein, as is reported to range from about 1 to 7 kJ/mol.[46] Additionally, the activation energy for the rupture of a hydrogen bond in an α-helix is reported to be approximately 8 kJ/mol in water, based on simulation.[47] It should be noted that a recent paper studied the HDX of heme protein myoglobin and found that the HDX follows the EX_2 behavior even for proteins at temperatures up to about 80 °C that is much higher than the temperature used in this study.[45] Therefore, it is likely that the HDX of our protein may also follow the EX_2 behavior. However, as the protein used here is different, a future study is needed to determine this.

Numerous protein-based drug formulations include the excipient sodium chloride for a range of purposes.[33] Due to its widespread usage and likely subtle impact on protein stability than other salts,[2,32] there is interest in measuring any effects that sodium chloride may have on the long-time HDX of BSA. Hence, HDX-SANS was performed on one sample containing 150 mM sodium chloride at 60 °C. This sample was measured first at 10 °C (Figure 2C) before increasing its temperature to 60 °C. The experimental procedure followed the same protocol used in the previous samples without NaCl. As with the previous samples, the kinetics SANS patterns of the sample containing NaCl also yield a downward shift in SANS pattern over time, as shown in the Supporting Information (S9).

Following the analysis approach outlined in the Materials and Methods Section, $R(Q)$ is obtained for the sample with NaCl. The results are shown in the Supporting Information (S10). The extracted values of y as a function of time elapsed are plotted along with the results for the sample without salt for comparison in Figure 8. The values of y for the sample with NaCl are consistently larger than those in D_2O without NaCl, measured at the same temperature. Thus, adding NaCl slightly slows the HDX at 60 °C. The fit parameters for the sample containing NaCl, also shown in Figure 6, agree with this observation and suggest that NaCl slightly reduces the rate of

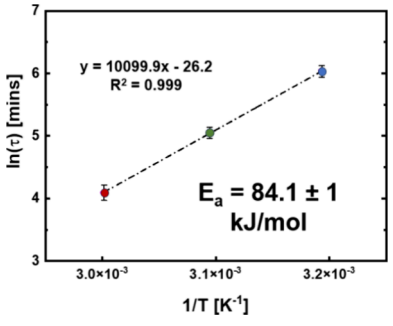

Figure 7. Plot of the natural log of τ for each sample, against the inverse of the sample temperature (40, 50, and 60 °C). The dotted line represents a linear fit of the data, with the fit equation displayed on the graph. From the slope of this fit, the activation energy, E_a, was calculated using the eq 8 and displayed on the graph.

https://doi.org/10.1021/acs.jpcb.4c03967
J. Phys. Chem. B XXXX, XXX, XXX−XXX

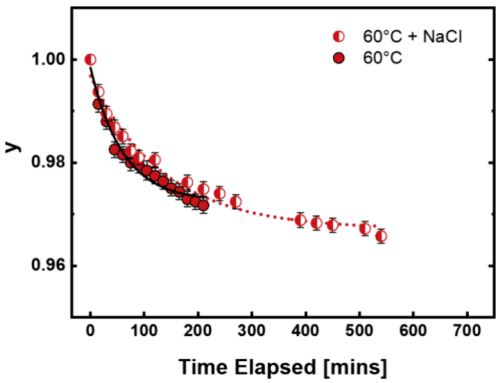

Figure 8. y for BSA sample exposed to 60 °C without any added salt (red circle) and with 150 mM sodium chloride (red half-filled circle) is plotted as a function of the time elapsed. Lines through the data points represent the model fitting with eq 7. The fit lines for sample exposed to 60 °C without any added salt and with 150 mM sodium chloride are the black solid line and red dotted line, respectively.

exchange and prevents some exchange during the heating stage, in comparison to the sample without added salt. This is consistent with the DSC result, as the addition of NaCl slightly increases the thermal stability of the sample. Therefore, our results indicate that even for BSA, which is dominated by α-helix secondary structures, there is agreement between the rate of HDX and thermal stability. This observation is in agreement with the previously reported results on NISTmAb, where the HDX rate for NISTmAb is correlated with the thermal stability in different salt formulations.[2] Therefore, combining the current result with the previous one, it is reasonable to believe that for most proteins, there is agreement between the exchange rate of long-time HDX and thermal stability.

The number of deuterons exchanged over time for each sample, with and without salt, is also extracted and is shown in Figure 9. The total number of exchangeable protons of one

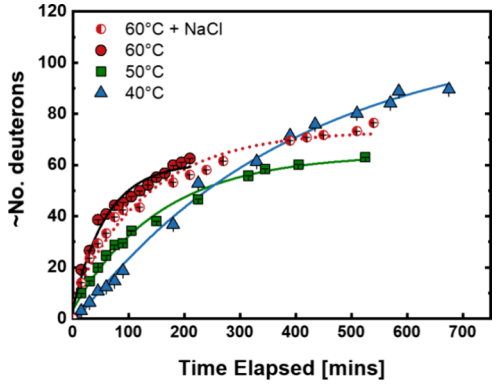

Figure 9. Number of deuterons incorporated into BSA as a function of time elapsed over the high temperature exposure for 60 °C (red circle); 60 °C + 150 mM sodium chloride (red half-filled circle); 50 °C (green square); and 40 °C (blue triangle). These values were calculated based on experimental results using eq 9.

BSA protein is about 1,060.[42] However, our samples were stored for about a week in D_2O at 10 °C before the HDX-SANS experiment to exchange the most labile hydrogens leaving the less accessible hydrogens to be probed by HDX-SANS. Based on a previous report, the core exchangeable protons, which are believed to be buried deep inside a protein, are about 143 for BSA.[42] The observed long-time HDX in our SANS experiments are likely related with these core exchangeable hydrogens, and the number exchanged during our experiment is a significant fraction of these buried but exchangeable hydrogens.

We can further estimate the number of exchanged hydrogens during the heating stage while the samples were heated from 10 °C to their respective target temperatures. After completion of kinetics measurements at their target temperature, all samples were measured again at 10 °C. Using the same ratio analysis method with these 10 °C data, the total number of exchanged protons for the sample exposed to 60 °C with added NaCl is 143 ± 1, which is in agreement with the previously reported estimated amount of core exchangeable hydrogens of BSA.[42] For the other samples, the total number of exchanged hydrogens is on the order of 200. Since the number of exchanged protons at 60 °C is about 70 (Figure 9), we can therefore estimate that 73 protons, or about half of total exchange, underwent HDX during the sample heating and cooling stage. It is reasonable to believe that during the cooling, the HDX is negligible. Thus, all 73 protons are exchanged during the heating process. Similarly, we also estimated the number of exchangeable hydrogens during high temperature exposure, based on the value of $1 - y_\infty$, as detailed in Table 3. Based on $1 - y_\infty$, there are about 73 deuterons

Table 3. Approximate Number of Deuterons Exchanged during the Heating Step from 10 °C to either 40 or 60 °C, Obtained from $R(Q)$ Measured at 10 °C

formulation conditions	measurement temperature [°C]	number of exchangeable hydrogens (based on $1 - y_\infty$)
D_2O	40	116 ± 1
D_2O	50	64 ± 1
D_2O	60	61 ± 1
D_2O + 150 mM NaCl	60	73 ± 1

available for exchange at 60 °C, which indicates that about 70 deuterons would have exchanged during heating alone, which is in reasonable agreement with the experimental estimated values from the discussion above.

CONCLUSIONS

HDX is known as a valuable method for assessing the dynamics and stability of secondary structures due to its association with the hydrogen bonds found in α-helices and β-sheets.[21,22] In this study, we apply the HDX-SANS to examine the HDX of BSA, a globular protein predominantly composed of α-helices, one of the most common secondary structural elements in proteins, while the previous HDX-SANS research focused on a β-sheet-rich protein (NISTmAb) with a Y-shaped quaternary structure in solution.[2]

Using HDX-SANS, we measured the HDX in the core of BSA proteins by allowing a few days of wait time for exposure of labile protons to solvent molecules prior to the HDX-SANS experiments. High-concentration BSA samples are studied over the range of 40 to 60 °C, and the kinetics of HDX are extracted as a function of the temperature. As expected, increasing the sample temperature significantly increased the HDX rate. Arrhenius behavior is observed for the temperature dependence of the exchange rate, from which the activation energy is extracted. Furthermore, the quantitative nature of SANS

https://doi.org/10.1021/acs.jpcb.4c03967
J. Phys. Chem. B XXXX, XXX, XXX−XXX

enables the in situ determination of the number of hydrogens exchanged as a function of time at the target temperature in formulation. We anticipate that the activation energies derived from HDX-SANS may prove useful as a quantitative metric for assessing the long-term stability of protein drug formulations and thus warrant more studies in the future.

The addition of NaCl, a common tonicity agent in formulation, is shown to have a slight stabilizing effect, with a small increase in the onset temperature of denaturation and slower rate of HDX. The decreased HDX rate by adding salts is associated with the increase in the onset temperature of denaturation of BSA. This result is consistent with previous observations for NISTmAb, a β-sheet-dominated protein, suggesting that the long-time HDX and thermal stability are intrinsically related, which may be a general behavior for proteins.

■ ASSOCIATED CONTENT

Supporting Information

The Supporting Information is available free of charge at https://pubs.acs.org/doi/10.1021/acs.jpcb.4c03967.

$R(Q)$ of 60 °C SANS measurements of BSA, with and without sodium chloride; sample of the data fitting performed to obtain values of y from $R(Q)$; residuals from the fitting of y over time; HDX-SANS patterns for the BSA sample with 150 mM sodium chloride; ratios for the sample containing sodium chloride; table of all values of y over time and table of all y_∞ (PDF)

■ AUTHOR INFORMATION

Corresponding Authors

Norman J. Wagner − *Department of Biomedical Engineering, College of Engineering and Center for Neutron Science, Department of Chemical and Biomolecular Engineering, College of Engineering, University of Delaware, Newark, Delaware 19711, United States;* orcid.org/0000-0001-9565-619X; Email: wagnernj@udel.edu

Yun Liu − *Center for Neutron Science, Department of Chemical and Biomolecular Engineering, College of Engineering, University of Delaware, Newark, Delaware 19711, United States; Center for Neutron Research, National Institute of Standards and Technology, Gaithersburg, Maryland 20899, United States;* orcid.org/0000-0002-0944-3153; Email: yunliu@nist.gov

Author

Róisín B. Donnelly − *Department of Biomedical Engineering, College of Engineering and Center for Neutron Science, Department of Chemical and Biomolecular Engineering, College of Engineering, University of Delaware, Newark, Delaware 19711, United States;* orcid.org/0000-0002-7519-946X

Complete contact information is available at: https://pubs.acs.org/10.1021/acs.jpcb.4c03967

Notes

The authors declare no competing financial interest.

■ ACKNOWLEDGMENTS

Funding for this research was provided by the National Science Foundation under award DMR-1935956. We would like to acknowledge IBBR for allowing us to use their equipment and Dr. Robert G. Brinson for his expert opinion regarding differential scanning calorimetry. Additionally, we acknowledge Dr. Kyle Anderson for providing expert opinions in hydrogen−deuterium exchange. We would like to acknowledge SASView and reference this website: http://www.sasview.org/. We would like to acknowledge Dr. Peter Gilbert for his contributions in the early stage of analysis development. Certain commercial equipment, instruments, or materials (or suppliers, or software, ...) are identified in this paper to foster understanding. Such identification does not imply recommendation or endorsement by the National Institute of Standards and Technology, nor does it imply that the materials or equipment identified are necessarily the best available for the purpose. Y.L. acknowledges the support provided by the Center for High Resolution Neutron Scattering, a partnership between the National Institute of Standards and Technology and the National Science Foundation under Agreement No. DMR-2010792.

■ ABBREVIATIONS

HDX, hydrogen−deuterium exchange; SANS, small-angle neutron scattering; MS, mass spectrometry; BSA, bovine serum albumin; DSC, differential scanning calorimetry

■ REFERENCES

(1) Urquhart, L. Top drugs and companies by sales in 2017. *Nat. Rev. Drug Discovery* **2018**, *17* (4), 232−232.

(2) Donnelly, R. B.; Pingali, S. V.; Heroux, L.; Brinson, R. G.; Wagner, N. J.; Liu, Y. Hydrogen−Deuterium Exchange Dynamics of NISTmAb Measured by Small Angle Neutron Scattering. *Mol. Pharmaceutics* **2023**, *20* (12), 6358−6367.

(3) Wang, W.; Singh, S.; Zeng, D. L.; King, K.; Nema, S. Antibody structure, instability, and formulation. *J. Pharm. Sci.* **2007**, *96* (1), 1−26.

(4) Le Basle, Y.; Chennell, P.; Tokhadze, N.; Astier, A.; Sautou, V. Physicochemical Stability of Monoclonal Antibodies: A Review. *J. Pharm. Sci.* **2020**, *109* (1), 169−190.

(5) Cho, E.; Mayhugh, B. M.; Srinivasan, J. M.; Sacha, G. A.; Nail, S. L.; Topp, E. M. Stability of antibody drug conjugate formulations evaluated using solid-state hydrogen-deuterium exchange mass spectrometry. *J. Pharm. Sci.* **2021**, *110* (6), 2379−2385.

(6) Moorthy, B. S.; Zarraga, I. E.; Kumar, L.; Walters, B. T.; Goldbach, P.; Topp, E. M.; Allmendinger, A. Solid-State Hydrogen−Deuterium Exchange Mass Spectrometry: Correlation of Deuterium Uptake and Long-Term Stability of Lyophilized Monoclonal Antibody Formulations. *Mol. Pharmaceutics* **2018**, *15* (1), 1−11.

(7) Gamage, C. L. D.; Hageman, T. S.; Weis, D. D. Rapid Prediction of Deamidation Rates of Proteins to Assess Their Long-Term Stability Using Hydrogen Exchange-Mass Spectrometry. *J. Pharm. Sci.* **2019**, *108* (6), 1964−1972.

(8) Masson, G. R.; Burke, J. E.; Ahn, N. G.; Anand, G. S.; Borchers, C.; Brier, S.; Bou-Assaf, G. M.; Engen, J. R.; Englander, S. W.; Faber, J.; et al. Recommendations for performing, interpreting and reporting hydrogen deuterium exchange mass spectrometry (HDX-MS) experiments. *Nat. Methods* **2019**, *16* (7), 595−602.

(9) Trabjerg, E.; Nazari, Z. E.; Rand, K. D. Conformational analysis of complex protein states by hydrogen/deuterium exchange mass spectrometry (HDX-MS): Challenges and emerging solutions. *TrAC Trends in Analytical Chemistry* **2018**, *106*, 125−138.

(10) Narang, D.; Lento, C.; J. Wilson, D. HDX-MS: An Analytical Tool to Capture Protein Motion in Action. *Biomedicines* **2020**, *8* (7), 224.

(11) Englander, J. J.; Del Mar, C.; Li, W.; Englander, S. W.; Kim, J. S.; Stranz, D. D.; Hamuro, Y.; Woods, V. L. Protein structure change studied by hydrogen-deuterium exchange, functional labeling, and

mass spectrometry. *Proc. Natl. Acad. Sci. U. S. A.* **2003**, *100* (12), 7057−7062.
(12) Majumdar, R.; Manikwar, P.; Hickey, J. M.; Samra, H. S.; Sathish, H. A.; Bishop, S. M.; Middaugh, C. R.; Volkin, D. B.; Weis, D. D. Effects of Salts from the Hofmeister Series on the Conformational Stability, Aggregation Propensity, and Local Flexibility of an IgG1Monoclonal Antibody. *Biochemistry* **2013**, *52* (19), 3376−3389.
(13) Wu, S.; Nguyen, T.; Moroz, O. V.; Turkenburg, J. P.; Nielsen, J. E.; Wilson, K. S.; Rand, K. D.; Teilum, K. Conformational heterogeneity of Savinase from NMR. *HDX-MS and X-ray diffraction analysis. PeerJ.* **2020**, *8*, No. e9408.
(14) Jia, R.; Martens, C.; Shekhar, M.; Pant, S.; Pellowe, G. A.; Lau, A. M.; Findlay, H. E.; Harris, N. J.; Tajkhorshid, E.; Booth, P. J.; Politis, A. Hydrogen-deuterium exchange mass spectrometry captures distinct dynamics upon substrate and inhibitor binding to a transporter. *Nat. Commun.* **2020**, *11* (1), 6162.
(15) Chu, I. T.; Pielak, G. J. Using NMR-detected hydrogen-deuterium exchange to quantify protein stability in cosolutes, under crowded conditions in vitro and in cells. *Magnetic Resonance Letters* **2023**, 3 (4), 319−326.
(16) Di Muzio, M.; Wildner, S.; Huber, S.; Hauser, M.; Vejvar, E.; Auzinger, W.; Regl, C.; Laimer, J.; Zennaro, D.; Wopfer, N.; Huber, C. G.; van Ree, R.; Mari, A.; Lackner, P.; Ferreira, F.; Schubert, M.; Gadermaier, G. Hydrogen/deuterium exchange memory NMR reveals structural epitopes involved in IgE cross-reactivity of allergenic lipid transfer proteins. *J. Biol. Chem.* **2020**, *295* (51), 17398−17410.
(17) Peacock, R. B.; Komives, E. A. Hydrogen/Deuterium Exchange and Nuclear Magnetic Resonance Spectroscopy Reveal Dynamic Allostery on Multiple Time Scales in the Serine Protease Thrombin. *Biochemistry* **2021**, *60* (46), 3441−3448.
(18) Dunkelberger, E. B.; Woys, A. M.; Zanni, M. T. 2D IR cross peaks reveal hydrogen-deuterium exchange with single residue specificity. *J. Phys. Chem. B* **2013**, *117* (49), 15297−305.
(19) Wang, R.; Mangion, I.; Makarov, A. A.; Kurouski, D. Use of Raman spectroscopy and size-exclusion chromatography coupled with HDX-MS spectroscopy for studying conformational changes of small proteins in solution. *J. Pharm. Biomed. Anal.* **2020**, *189*, No. 113399.
(20) Teixeira, S. C. M.; Leão, J. B.; Gagnon, C.; McHugh, M. A. High pressure cell for Bio-SANS studies under sub-zero temperatures or heat denaturing conditions. *J. Neutron Res.* **2018**, 13−23.
(21) Pan, J.; Han, J.; Borchers, C. H.; Konermann, L. Hydrogen/Deuterium Exchange Mass Spectrometry with Top-Down Electron Capture Dissociation for Characterizing Structural Transitions of a 17 kDa Protein. *J. Am. Chem. Soc.* **2009**, *131* (35), 12801−12808.
(22) Konermann, L.; Pan, J.; Liu, Y.-H. Hydrogen exchange mass spectrometry for studying protein structure and dynamics. *Chem. Soc. Rev.* **2011**, *40* (3), 1224−1234.
(23) Lu, R.; Li, W.-W.; Katzir, A.; Raichlin, Y.; Yu, H.-Q.; Mizaikoff, B. Probing the secondary structure of bovine serum albumin during heat-induced denaturation using mid-infrared fiberoptic sensors. *Analyst* **2015**, *140* (3), 765−770.
(24) Molodenskiy, D.; Shirshin, E.; Tikhonova, T.; Gruzinov, A.; Peters, G.; Spinozzi, F. Thermally induced conformational changes and protein−protein interactions of bovine serum albumin in aqueous solution under different pH and ionic strengths as revealed by SAXS measurements. *Phys. Chem. Chem. Phys.* **2017**, *19* (26), 17143−17155.
(25) Murayama, K.; Tomida, M. Heat-Induced Secondary Structure and Conformation Change of Bovine Serum Albumin Investigated by Fourier Transform Infrared Spectroscopy. *Biochemistry* **2004**, *43* (36), 11526−11532.
(26) Bulone, D.; Martorana, V.; San Biagio, P. L. Effects of intermediates on aggregation of native bovine serum albumin. *Biophys. Chem.* **2001**, *91* (1), 61−69.
(27) Su, R.; Qi, W.; He, Z.; Zhang, Y.; Jin, F. Multilevel structural nature and interactions of bovine serum albumin during heat-induced aggregation process. *Food Hydrocolloids* **2008**, *22* (6), 995−1005.
(28) Yadav, P.; Yadav, A. B. Preparation and characterization of BSA as a model protein loaded chitosan nanoparticles for the development of protein-/peptide-based drug delivery system. *Future J. Pharm. Sci.* **2021**, *7* (1), 200.
(29) Al-Husseini, J. K.; Stanton, N. J.; Selassie, C. R. D.; Johal, M. S. The Binding of Drug Molecules to Serum Albumin: The Effect of Drug Hydrophobicity on Binding Strength and Protein Desolvation. *Langmuir* **2019**, *35* (52), 17054−17060.
(30) James, E. I.; Murphree, T. A.; Vorauer, C.; Engen, J. R.; Guttman, M. Advances in Hydrogen/Deuterium Exchange Mass Spectrometry and the Pursuit of Challenging Biological Systems. *Chem. Rev.* **2022**, *122* (8), 7562−7623.
(31) Parmar, A. S.; Muschol, M. Hydration and Hydrodynamic Interactions of Lysozyme: Effects of Chaotropic versus Kosmotropic Ions. *Biophys. J.* **2009**, *97* (2), 590−598.
(32) Gregory, K. P.; Elliott, G. R.; Robertson, H.; Kumar, A.; Wanless, E. J.; Webber, G. B.; Craig, V. S. J.; Andersson, G. G.; Page, A. J. Understanding specific ion effects and the Hofmeister series. *Phys. Chem. Chem. Phys.* **2022**, *24* (21), 12682−12718.
(33) Ghosh, I.; Gutka, H.; Krause, M. E.; Clemens, R.; Kashi, R. S. A systematic review of commercial high concentration antibody drug products approved in the US: formulation composition, dosage form design and primary packaging considerations. *MAbs* **2023**, *15* (1), 2205540.
(34) Wang, S. S.; Yan, Y. S.; Ho, K. US FDA-approved therapeutic antibodies with high-concentration formulation: summaries and perspectives. *Antib Ther* **2021**, *4* (4), 262−272.
(35) Zhang, F.; Roosen-Runge, F.; Skoda, M.; Jacobs, R.; Wolf, M.; Callow, P.; Frielinghaus, H.; Pipich, V.; Prévost, S.; Schreiber, F. Hydration and interactions in protein solutions containing concentrated electrolytes studied by small-angle scattering. *Physical chemistry chemical physics: PCCP* **2012**, *14*, 2483−93.
(36) Yearley, E. J.; Zarraga, I. E.; Shire, S. J.; Scherer, T. M.; Gokarn, Y.; Wagner, N. J.; Liu, Y. Small-angle neutron scattering characterization of monoclonal antibody conformations and interactions at high concentrations. *Biophys. J.* **2013**, *105* (3), 720−31.
(37) Kotlarchyk, M.; Chen, S. H. Analysis of Small-Angle Neutron-Scattering Spectra from Polydisperse Interacting Colloids. *J. Chem. Phys.* **1983**, *79* (5), 2461−2469.
(38) Bendedouch, D.; Chen, S. H. Structure and interparticle interactions of bovine serum albumin in solution studied by small-angle neutron scattering. *J. Phys. Chem.* **1983**, *87* (9), 1473−1477.
(39) Giancola, C.; De Sena, C.; Fessas, D.; Graziano, G.; Barone, G. DSC studies on bovine serum albumin denaturation. Effects of ionic strength and SDS concentration. *Int. J. Biol. Macromol.* **1997**, *20* (3), 193−204.
(40) Gumpen, S.; Hegg, P. O.; Martens, H. Thermal stability of fatty acid-serum albumin complexes studied by differential scanning calorimetry. *Biochimica et Biophysica Acta (BBA) - Lipids and Lipid Metabolism* **1979**, *574* (2), 189−196.
(41) Oganesyan, I.; Lento, C.; Wilson, D. J. Contemporary hydrogen deuterium exchange mass spectrometry. *Methods* **2018**, *144*, 27−42.
(42) Rosenberg, A.; Chakravarti, K. Studies of Hydrogen Exchange in Proteins: I. The Exchange Kinetics of Bovine Carbonic Anhydrase. *J. Biol. Chem.* **1968**, *243* (19), 5193−5201.
(43) Hodge, E. A.; Benhaim, M. A.; Lee, K. K. Bridging protein structure, dynamics, and function using hydrogen/deuterium-exchange mass spectrometry. *Protein Sci.* **2020**, *29* (4), 843−855.
(44) Hodkinson, J. P.; Jahn, T. R.; Radford, S. E.; Ashcroft, A. E. HDX-ESI-MS Reveals Enhanced Conformational Dynamics of the Amyloidogenic Protein β2-Microglobulin upon Release from the MHC-1. *J. Am. Soc. Mass Spectrom.* **2009**, *20* (2), 278−286.
(45) Tajoddin, N. N.; Konermann, L. Analysis of Temperature-Dependent H/D Exchange Mass Spectrometry Experiments. *Anal. Chem.* **2020**, *92* (14), 10058−10067.
(46) Williams, D. H.; Searle, M. S.; Mackay, J. P.; Gerhard, U.; Maplestone, R. A. Toward an estimation of binding constants in aqueous solution: studies of associations of vancomycin group antibiotics. *Proc. Natl. Acad. Sci. U. S. A.* **1993**, *90* (4), 1172−1178.

https://doi.org/10.1021/acs.jpcb.4c03967
J. Phys. Chem. B XXXX, XXX, XXX−XXX

812 (47) Sheu, S.-Y.; Yang, D.-Y.; Selzle, H. L.; Schlag, E. W. Energetics
813 of hydrogen bonds in peptides. *Proc. Natl. Acad. Sci. U. S. A.* **2003**,
814 *100* (22), 12683−12687.

https://doi.org/10.1021/acs.jpcb.4c03967
J. Phys. Chem. B XXXX, XXX, XXX−XXX